arXiv:1201.1234v1 [hep-th] 5 Jan 2012

WKB Analysis of $\mathcal{PT}$-Symmetric Sturm-Liouville problems

Carl M. Bender[1*] and Hugh F. Jones[2†]

[1] *Department of Physics, Kings College London, Strand, London WC2R 1LS, UK* [‡]
[2] *Blackett Laboratory, Imperial College, London SW7 2AZ, UK*

Most studies of $\mathcal{PT}$-symmetric quantum-mechanical Hamiltonians have considered the Schrödinger eigenvalue problem on an infinite domain. This paper examines the consequences of imposing the boundary conditions on a finite domain. As is the case with regular Hermitian Sturm-Liouville problems, the eigenvalues of the $\mathcal{PT}$-symmetric Sturm-Liouville problem grow like n^2 for large n. However, the novelty is that a $\mathcal{PT}$ eigenvalue problem on a finite domain typically exhibits a sequence of critical points at which pairs of eigenvalues cease to be real and become complex conjugates of one another. For the potentials considered here this sequence of critical points is associated with a turning point on the imaginary axis in the complex plane. WKB analysis is used to calculate the asymptotic behaviors of the real eigenvalues and the locations of the critical points. The method turns out to be surprisingly accurate even at low energies.

PACS numbers: 11.30.Er, 02.30.Em, 03.65.-w

I. INTRODUCTION

This paper uses WKB analysis to examine the approximate solutions of complex non-Hermitian $\mathcal{PT}$-symmetric Sturm-Liouville eigenvalue problems on finite domains. These problems are qualitatively different from ordinary Hermitian eigenvalue problems because, as we will show, there is a sequence of critical points at which the eigenvalues become pairwise complex. WKB provides an extremely accurate asymptotic approximation to the locations of these critical points.

A conventional Sturm-Liouville eigenvalue problem in Schrödinger form is a second-order differential equation

$$-\psi''(x) + V(x)\psi(x) = \lambda\psi(x), \tag{1}$$

where λ is the eigenvalue, accompanied by a set of homogeneous boundary conditions

$$\psi(a) = 0, \qquad \psi(b) = 0. \tag{2}$$

If a and b are finite and the potential $V(x)$ is real and smooth for $a \leq x \leq b$, then this eigenvalue problem is said to be a *regular* Sturm-Liouville problem.

WKB theory gives a good approximation to the solution of this problem for large eigenvalues λ [1]. Equation (2) takes the form $\psi''(x) + Q(x)\psi(x) = 0$, where $Q(x) = \lambda - V(x)$,

[‡] Permanent address: Department of Physics, Washington University, St. Louis, MO 63130, USA.
*Electronic address: cmb@wustl.edu
†Electronic address: h.f.jones@imperial.ac.uk

and if $\lambda \gg 1$, we may assume that $Q(x) \neq 0$ on the interval $a \leq x \leq b$. Thus, there are no turning points. When $\lambda \gg 1$, the WKB approximation satisfying $\psi(a) = 0$,

$$\psi(x) \sim \frac{C}{[Q(x)]^{1/4}} \sin\left[\int_a^x ds\, \sqrt{\lambda - V(s)}\right], \tag{3}$$

is uniformly valid over the entire interval. Imposing the boundary condition $\psi(b) = 0$ then gives the eigenvalue condition

$$\int_a^b ds\, \sqrt{\lambda_n - V(s)} \sim n\pi \quad (n = 1, 2, 3, \ldots). \tag{4}$$

For large λ this gives an accurate asymptotic approximation to the eigenvalues:

$$\lambda_n \sim \frac{n^2\pi^2}{(a-b)^2} \quad (n \to \infty). \tag{5}$$

Note that the eigenvalues grow like n^2 for large n. This result is general and holds for all regular Sturm-Liouville eigenvalue problems because to leading order in the WKB approximation the eigenvalues become insensitive to the potential $V(x)$ and thus the eigenvalues approach those of a square-well potential.

In this paper we study the complex $\mathcal{PT}$-symmetric version of the eigenvalue problem in (1) and (2). Now, instead of the potential being real, the eigenvalue problem takes the form

$$-\psi''(x) - gV(ix)\psi(x) = \lambda\psi(x), \tag{6}$$

where g is a coupling constant and $V(x)$ is a real function of its argument. In order to respect the $\mathcal{PT}$ symmetry, the boundary conditions are imposed on the real-x axis at parity-symmetric points:

$$\psi(\pm 1) = 0. \tag{7}$$

We will see that WKB provides an excellent asymptotic solution to this problem for large λ but that one-turning-point analysis is required.

Eigenvalue problems like this have already been studied numerically in the literature in a variety of physical contexts. An example of a $\mathcal{PT}$-symmetric Hamiltonian having a complex Sturm-Liouville eigenvalue problem like that in (6) and (7) was first discussed by Günther, Znojil, and Wu [2] in the context of the Squire equation of hydrodynamics. Essentially the same Hamiltonian and boundary conditions occur in the context of superconducting wires[3], and again in a different guise in the consideration of the magnetic resonance signal of spin-polarized Rb atoms near the surfaces of coated cells [4]. The Schrödinger eigenvalue equation of Ref. [3],

$$-\psi''(x) - iIx\psi(x) = \lambda\psi(x), \tag{8}$$

is posed on the finite domain $|x| \leq 1$ with homogeneous boundary conditions $\psi(\pm 1) = 0$. The eigenvalues λ are plotted in Fig. 1 as functions of the real coupling constant I. Observe that when $0 \leq I \leq 12.31$, the eigenvalues are all real. This parametric region is called the region of *unbroken* $\mathcal{PT}$ symmetry. However, as I reaches the critical value 12.31, the two lowest eigenvalues become degenerate, and as I increases past 12.31, these eigenvalues split into a complex-conjugate pair. Thus, for $I > 12.31$ the eigenspectrum is no longer entirely real. As I continues to increase, more and more pairs of real eigenvalues become degenerate

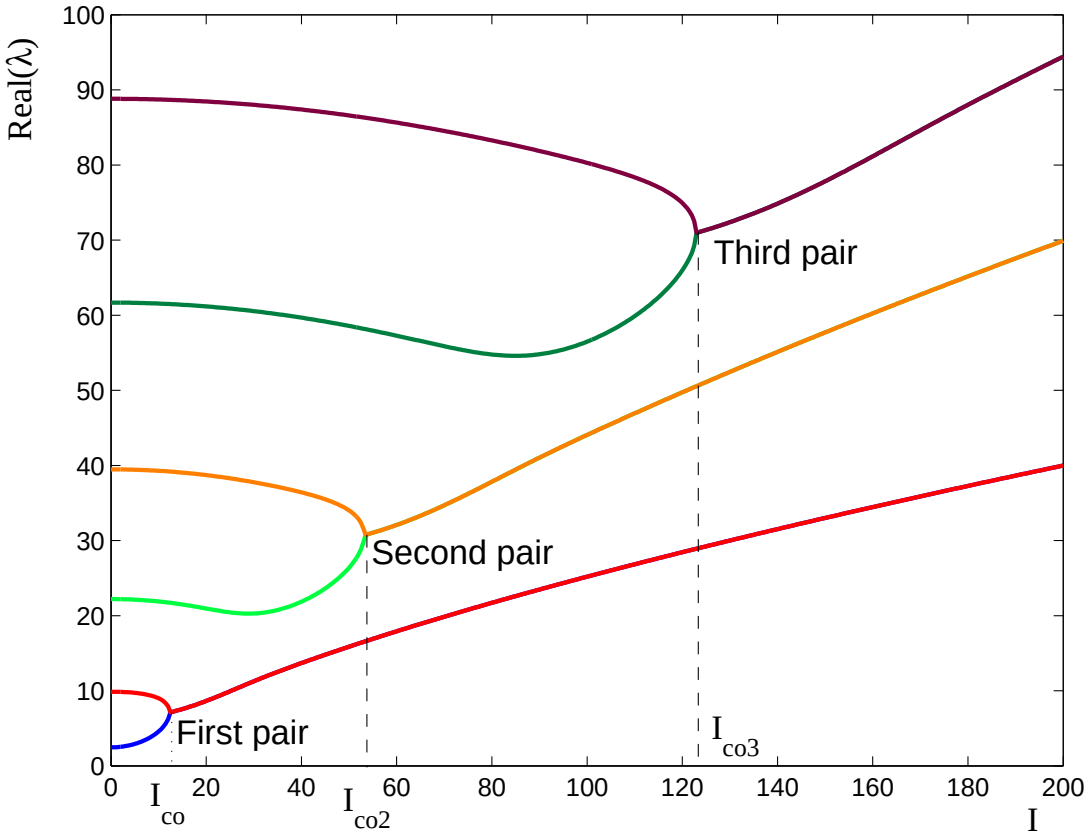

FIG. 1: (Color on line) Real parts of eigenvalues of the $\mathcal{PT}$-symmetric eigenvalue problem (8), taken from Ref. [3].

and split into complex-conjugate pairs. The critical values of a coupling constant at which the eigenvalues become degenerate are often called *exceptional points* [5]-[10].

Another example of a $\mathcal{PT}$-symmetric Hamiltonian giving rise to a Sturm-Liouville eigenvalue problem on a finite domain is

$$H = -\frac{d^2}{d\theta^2} + ig\cos\theta, \tag{9}$$

where g is a real parameter [11]. Here, the eigenfunctions are required to be 2π periodic and odd in θ. The region of unbroken $\mathcal{PT}$ symmetry is $|g| < 3.4645$ [11] (see Fig. 2). Note that the behavior of the eigenvalues is virtually identical to that shown in Fig. 1. It is this feature that motivated us to use WKB analysis to investigate these problems in a more general context.

This paper is organized simply. In Sec. II we describe the WKB calculation, culminating in Eq. (32), which is our principal result. Sec. III gives numerical results based on (32) for a variety of Hamiltonians, including in particular those of (8) and (9). Section IV contains some brief concluding remarks.

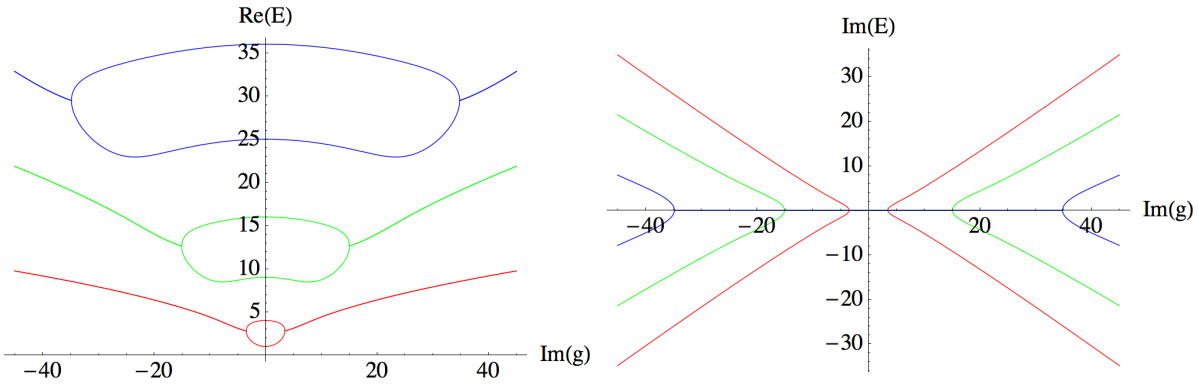

FIG. 2: Real and imaginary parts of eigenvalues of the $\mathcal{PT}$-symmetric Hamiltonian (9), taken from Ref. [11]. The region of unbroken $\mathcal{PT}$ symmetry is $|g| < 3.4645$.

II. WKB CALCULATION OF EIGENVALUES AND CRITICAL POINTS

Our objective is to find accurate asymptotic approximations to the eigenvalues λ in (6) for large λ and hence to determine approximately the critical values of g. In our WKB approximation we treat both the eigenvalues λ and the associated values of g as large and proportional. Thus, we begin by substituting

$$\lambda = ag. \tag{10}$$

The eigenvalue equation (6) then takes the form

$$\psi''(x) = -gQ(x)\psi(x), \tag{11}$$

where $Q(x) = V(ix) + a$.

We will see that for large λ, the asymptotic solution to (11) is controlled by a turning point on the imaginary-x axis at $x = ib$, where b satisfies the equation

$$V(-b) + a = 0. \tag{12}$$

Near the turning point at ib, we write x as $x = ib + yc$, where $y \ll 1$. Thus, a one-term Taylor approximation to $Q(x)$ near ib is $Q(x) \sim iycV'(-b)$, and the differential equation (11) is approximately

$$\frac{d^2}{dy^2}\psi(y) = -igc^3V'(-b)y\psi(y). \tag{13}$$

We then convert (13) to the standard Airy differential equation

$$\frac{d^2}{dy^2}\psi(y) = y\psi(y) \tag{14}$$

by setting

$$c = \gamma e^{i\pi/6}, \tag{15}$$

where $\gamma = [gV'(-b)]^{-1/3}$ is real. By choosing the sign of g appropriately, we may take γ to be positive. The relationship between the x and y variables is given explicitly by

$$y = \frac{x - ib}{\gamma}e^{-i\pi/6}. \tag{16}$$

Two linearly independent solutions to the Airy equation (14) are $\mathrm{Ai}(y)$ and $\mathrm{Ai}(\omega y)$, where $\omega = e^{2\pi i/3}$ is a cube root of unity. Hence, the general solution to (14) is

$$\psi(y) = K_1 \mathrm{Ai}(y) + K_2 \mathrm{Ai}(\omega y), \tag{17}$$

where K_1 and K_2 are arbitrary constants. Thus, near the turning point at $x = ib$ on the imaginary axis, the solution $\psi(x)$ to the Schrödinger equation (11) is

$$\psi(x) \sim K_1 \mathrm{Ai}\left(\frac{x-ib}{\gamma} e^{-i\pi/6}\right) + K_2 \mathrm{Ai}\left(\omega \frac{x-ib}{\gamma} e^{-i\pi/6}\right). \tag{18}$$

Away from the turning point at $x = ib$ the solution to (11) can be expressed in terms of WKB functions because $g \gg 1$. When $\mathrm{Re}\, x < 0$, the WKB approximation to $\psi(x)$ on the left takes the form

$$\psi_L(x) \sim \frac{L_1}{[Q(x)]^{1/4}} \exp\left[i \int_x^{ib} ds\, \sqrt{gQ(s)}\right] + \frac{L_2}{[Q(x)]^{1/4}} \exp\left[-i \int_x^{ib} ds\, \sqrt{gQ(s)}\right], \tag{19}$$

and when $\mathrm{Re}\, x > 0$, the WKB approximation on the right is

$$\psi_R(x) \sim \frac{R_1}{[Q(x)]^{1/4}} \exp\left[i \int_{ib}^{x} ds\, \sqrt{gQ(s)}\right] + \frac{R_2}{[Q(x)]^{1/4}} \exp\left[-i \int_{ib}^{x} ds\, \sqrt{gQ(s)}\right], \tag{20}$$

where L_1, L_2, R_1, and R_2 are arbitrary constants. Note that the sense of integration in (19) and (20) is from left to right; in (19) the integration is rightward and towards the turning point at ib and in (20) the integration is rightward and away from the turning point.

We must now find equations that relate the six constants in the approximations to $\psi(x)$ in (17) - (20). Imposing the boundary condition $\psi_L(-1) = 0$ on $\psi_L(x)$ in (19), we obtain a condition relating L_1 and L_2,

$$0 = L_1 \exp\left[i \int_{-1}^{ib} ds\, \sqrt{gQ(s)}\right] + L_2 \exp\left[-i \int_{-1}^{ib} ds\, \sqrt{gQ(s)}\right], \tag{21}$$

and imposing the boundary condition $\psi_R(1) = 0$ on $\psi_R(x)$ in (20), we obtain a condition relating R_1 and R_2,

$$0 = R_1 \exp\left[i \int_{ib}^{1} ds\, \sqrt{gQ(s)}\right] + R_2 \exp\left[-i \int_{ib}^{1} ds\, \sqrt{gQ(s)}\right]. \tag{22}$$

Four additional conditions relating the constants can be found by matching asymptotically the WKB approximations (19) and (20) to the Airy approximation (17) or (18) near the turning point. To perform the match, we must show that in an overlap region near the turning point, further asymptotic approximations to each of the asymptotic approximations that we have already found are identical. We will need to use two approximations to the Airy function for large argument that are valid in the appropriate Stokes' wedges [1]:

$$\mathrm{Ai}(z) \sim \frac{1}{2\sqrt{\pi}} z^{-1/4} \exp\left(-\frac{2}{3} z^{3/2}\right) \quad (|z| \gg 1,\ |\arg z| < \pi) \tag{23}$$

and

$$\mathrm{Ai}(-z) \sim \frac{1}{\sqrt{\pi}} z^{-1/4} \sin\left(\frac{2}{3} z^{3/2} + \frac{\pi}{4}\right) \quad \left[|z| \gg 1,\ |\arg(-z) < \frac{2\pi}{3}\right]. \tag{24}$$

We will perform the asymptotic match in the y variable. Because $y = (x - ib)/c$ and $c = \mathrm{O}\left(g^{-1/3}\right)$ is small for large g, it follows that when x is near ib, y may be treated as large. Thus, it is valid to use the asymptotic approximations (23) and (24) for the Airy functions.

First, we examine the WKB approximation $\psi_R(x)$ in (20). This WKB approximation is valid in the right-half x plane away from the turning point at ib; that is, outside the small circle in Fig. 3. From the asymptotic approximations

$$\begin{aligned} \int_{ib}^{x} ds\, \sqrt{gQ(s)} &\sim \frac{2}{3} i y^{3/2}, \\ [Q(x)]^{-1/4} &\sim g^{1/4} \gamma^{1/2} e^{-i\pi/6} y^{-1/4}, \end{aligned} \tag{25}$$

the asymptotic approximation to the WKB approximation to $\psi_R(x)$ in (20) becomes

$$\psi_R(x) \sim g^{1/4} \gamma^{1/2} e^{-i\pi/6} y^{-1/4} \left[R_1 \exp\left(-\frac{2}{3} y^{3/2} \right) + R_2 \exp\left(\frac{2}{3} y^{3/2} \right) \right]. \tag{26}$$

This approximation is valid as we approach the circle from the outside.

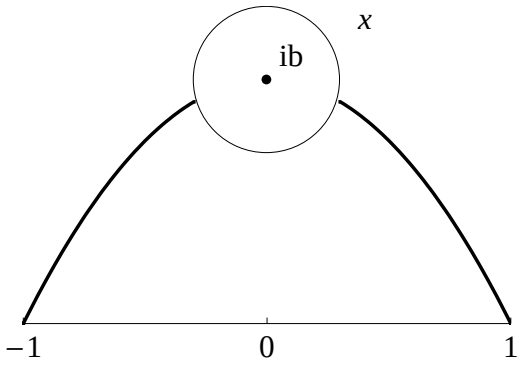

FIG. 3: Schematic path for the WKB integral from the end points $x = \pm 1$ via the turning point at $x = ib$. Inside the circle, very close to the turning point, the WKB approximation must be matched on either side with the asymptotic approximation to the Airy solution.

The left panel of Fig. 4 shows the complex-x plane and the right panel shows the corresponding complex-y plane in the vicinity of the turning point at $x = ib$. From (16), we see that the complex-y plane is rotated by $-30°$ relative to the complex-x plane. The Airy functions in (17) are oscillatory along the wiggly lines in the right panel.

The Airy function approximation in (17) is valid inside the circle in Fig. 3. We must match the WKB approximation in (26) to the Airy approximation along the solid line (R) in the left panel of Fig. 4. This line corresponds to the two wiggly lines marked (R) in the right panel. Because both wiggly lines satisfy the conditions of (23), as we approach the right edge of the circle from inside, we use only this asymptotic approximation to obtain

$$\psi(x) \sim \frac{1}{2\sqrt{\pi}} y^{-1/4} \left[K_1 \exp\left(-\frac{2}{3} y^{3/2} \right) + K_2 \exp\left(\frac{2}{3} y^{3/2} - \frac{i\pi}{6} \right) \right]. \tag{27}$$

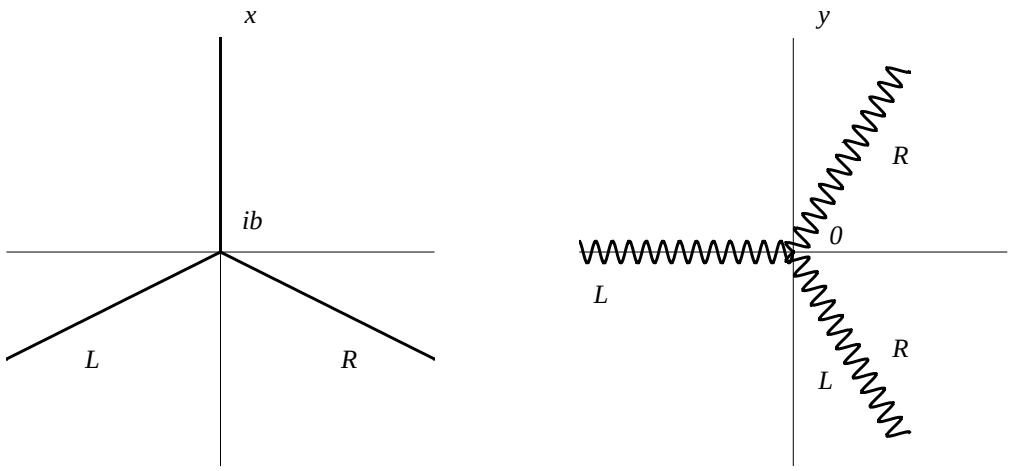

FIG. 4: Matching paths in the complex-x plane (left panel) and y plane (right panel).

This asymptotic match produces two algebraic equations for the coefficients:

$$\begin{aligned} \frac{K_1}{2\sqrt{\pi}} &= R_1 g^{1/4}\gamma^{1/2}e^{-i\pi/6}, \\ \frac{K_2}{2\sqrt{\pi}} &= R_2 g^{1/4}\gamma^{1/2}. \end{aligned} \tag{28}$$

Next, we further approximate the WKB approximation in (19). Again, using the formulas in (25), we find that in the left-half x plane

$$\psi_L(x) \sim g^{1/4}\gamma^{1/2}e^{i\pi/3}(-y)^{-1/4}\left[L_1\exp\left(\frac{2}{3}i(-y)^{3/2}\right) + L_2\exp\left(-\frac{2}{3}i(-y)^{3/2}\right)\right]. \tag{29}$$

For the Airy approximation (17) we must now perform the asymptotic match along the solid line (L) in the left panel of Fig. 4. This line corresponds to the two wiggly lines marked (L) in the right panel. In this case the wiggly line along the negative-y axis requires that we use the asymptotic approximation (24) for the Airy function $\mathrm{Ai}(y)$. For the other Airy function $\mathrm{Ai}(\omega y)$ we use the asymptotic approximation (23). This allows us to obtain the following asymptotic approximation to the Airy-function approximation to $\psi(x)$ in (17):

$$\psi(x) \sim \frac{K_1}{\sqrt{\pi}}(-y)^{-1/4}\sin\left[\frac{2}{3}(-y)^{3/2}+\frac{\pi}{4}\right] + \frac{K_2}{2\sqrt{\pi}}(-y)^{-1/4}e^{i\pi/12}\exp\left[\frac{2}{3}i(-y)^{3/2}\right]. \tag{30}$$

This asymptotic match produces two further algebraic equations

$$\begin{aligned} \frac{K_1}{2\sqrt{\pi}} &= L_2 g^{1/4}\gamma^{1/2}e^{-i\pi/6}, \\ \frac{1}{2\sqrt{\pi}}\left(-K_1 e^{2i\pi/3}+K_2\right) &= L_1 g^{1/4}\gamma^{1/2}. \end{aligned} \tag{31}$$

Finally, we combine all six algebraic equations (21), (22), (28), and (31), and obtain a secular equation that determines the eigenvalues:

$$\sin\left[\int_{-1}^{1} ds\,\sqrt{gQ(s)}\right] + \frac{1}{2}\exp\left[i\int_{-1}^{ib} ds\,\sqrt{gQ(s)} - i\int_{ib}^{1} ds\,\sqrt{gQ(s)}\right] = 0. \tag{32}$$

Equation (32) is our main result. This equation is *real*, which is a general feature of all $\mathcal{PT}$-symmetric secular equations [12]. To see that it is indeed real note that the argument of the sine can be written as $2\mathrm{Re}I_+$, while that of the exponential can be written as $2\ \mathrm{Im}I_+$, where $I_+ = \int_{ib}^{1} ds\ \sqrt{gQ(s)}$

The first term of (32) is what one would obtain from a path going directly along the real axis from $x = -1$ to $x = 1$ without going through the turning point at $x = ib$. This corresponds to the no-turning-point result of (3) for the Hermitian case. We shall see in the next section that this term by itself gives very little structure. The second term is the exponential of a generically large real number. When that number is large and negative it makes very little difference to the calculation of the eigenvalue, and when it is large and positive the equation has no real solutions because $|\sin\theta| < 1$. All the interesting structure, including the critical points, comes from the interplay of the two terms in the region where the exponent passes through a zero.

III. NUMERICAL CALCULATIONS

In Fig. 5 we show the predictions of (32) for the real eigenvalues of the Airy potential $V(ix) = ix$ occurring in (8) (with g taking the role of I). These are the solid lines, which are essentially indistinguishable from the numerical results of Fig. 1. Remarkably, the range of validity of the WKB approximation extends to small values of g and λ. In Fig. 5 we also show as dotted lines the result of the no-turning-point WKB approximation, namely the first term of (32). While this approximation reproduces correctly the square-well eigenvalues for $g = 0$, it fails to reproduce the interesting structure, which arises as a result of the interplay between both terms of (32). For this potential the full WKB approximation predicts that the critical points occur at $\lambda = g/\sqrt{3}$, which is actually an exact result [2, 13].

In Fig. 6 we show the analogous results for the sinusoidal potential in (9) (with $\theta = \pi/2 - x$). The same features of the approximation are true here too, and (32) reproduces very closely the numerical results of Fig. 2. The reason that the spectra of the two potentials in (8) and (9) are so close is that within the range of the integrals $\int ds\sqrt{gQ(s)}$ occurring in (32) the function $\sin s$ is well approximated by s. Note that in this case $b = \arcsin a$ is multivalued, so there is a series of turning points on the imaginary axis. For the WKB calculation we considered only the nearest turning point, which is close to ia.

In Fig. 7 we show the analogous results for the potential $V(ix) = i\sin(2x)$. Again, these are indistinguishable from numerical results obtained from a shooting method, but now they differ from the eigenvalues of the scaled Airy potential $V(ix) = 2ix$, which demonstrates that within the range of the integrals $\int ds\sqrt{gQ(s)}$ it is not valid to neglect the s^3 term in the expansion of $\sin(2s)$.

What happens if we apply our WKB approximation to the potential $V(ix) = -ix^3$? Now there are three complex turning points, which are located at $x = ib\{1, \omega, \omega^2\}$. Since our WKB analysis involved only one turning point, we chose a path going through the turning point at ib. The numerical results in Fig. 8 show a single low-energy critical point, which the WKB approximation fails to reproduce. In this case the second term of (32) is always negligible, so there is no effective interplay between the two terms. On the other hand, the first term tracks very well the curves for the higher energy levels. It is conceivable that a WKB path going through the other two turning points would reproduce the low-energy structure, and we intend to address this problem in a future publication.

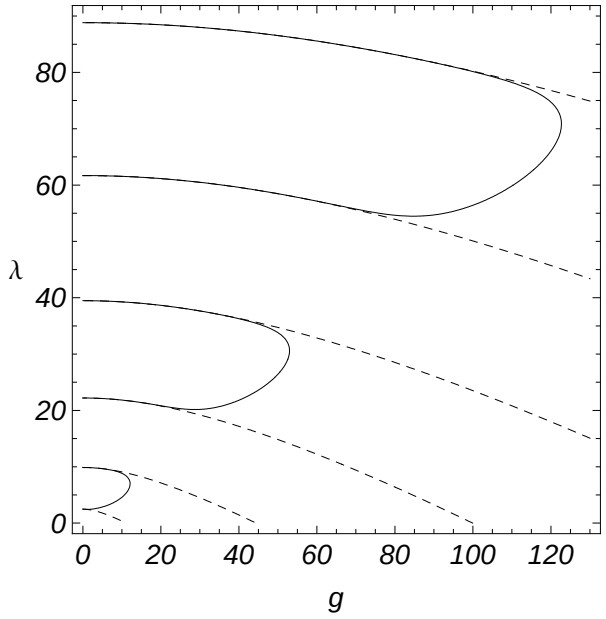

FIG. 5: WKB approximation for the real energy levels of the Airy potential $V(ix) = ix$. The no-turning-point approximation (dashed line), which is obtained by neglecting the second term of (32), exhibits no critical points. The full result (solid line), which includes the second term, indeed gives the critical points as a consequence of the interplay of the two terms. The solid line is essentially indistinguishable from the numerical results in Fig. 1, even at low energies.

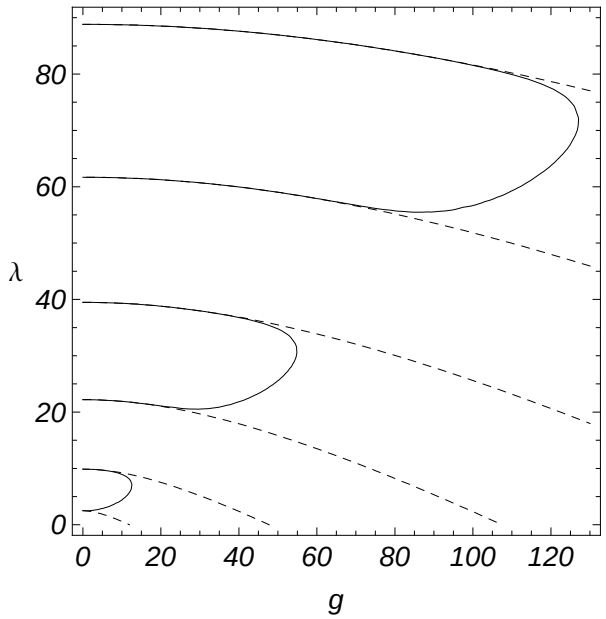

FIG. 6: WKB approximation for the real energy levels of the potential $V(ix) = i \sin x$. The notation is as in Fig. 5. The solid line is essentially indistinguishable from the numerical results in Fig. 2, even at low energies.

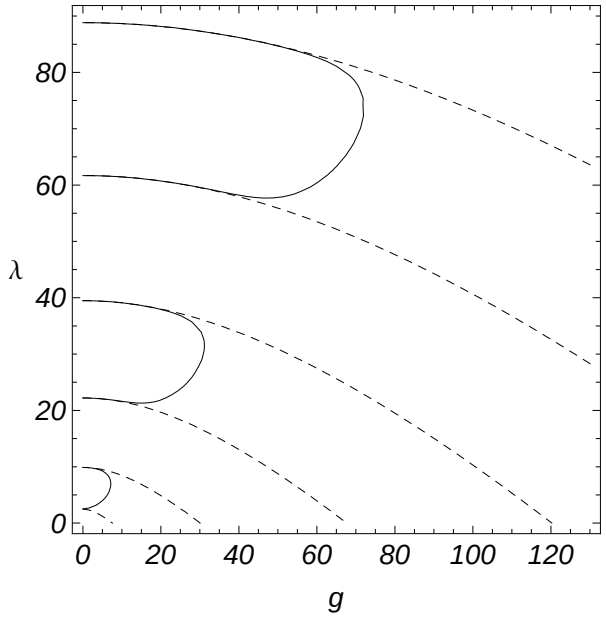

FIG. 7: WKB approximation for the real energy levels of the potential $V(ix) = i\sin(2x)$. These are distinct from those of the scaled Airy potential $V(ix) = 2ix$.

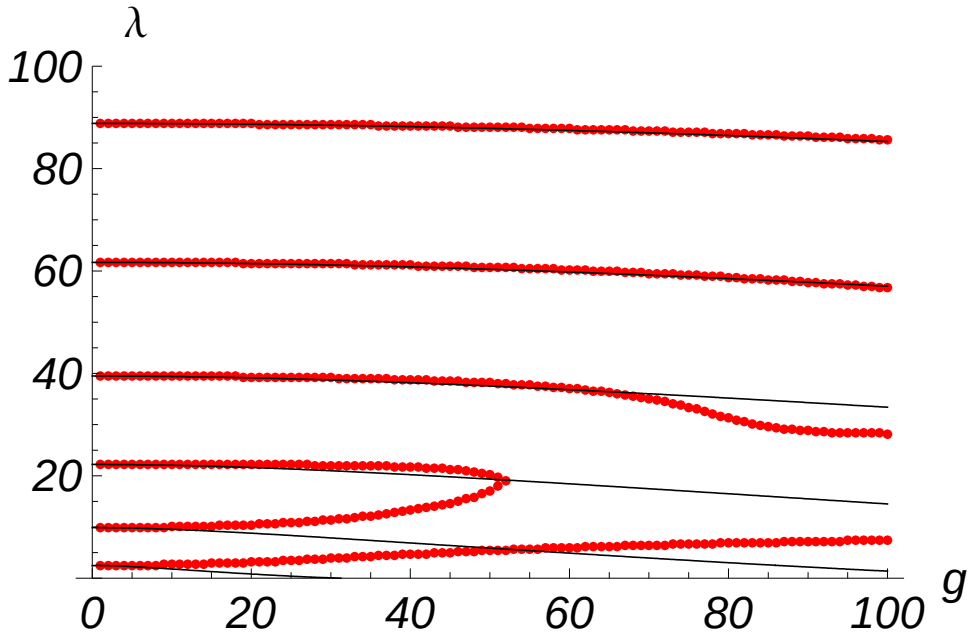

FIG. 8: (Color on line) WKB approximation for the real energy levels of the potential $V(ix) = -ix^3$ compared with the numerical results (red dots). The numerical results show just one low-energy critical point in the range of g considered, while the WKB approximation gives no critical points. This is because the second term of (32) is negligible in this case.

IV. COMMENTS AND DISCUSSION

In this paper we have used WKB analysis to derive the simple formula (32), which gives an extremely accurate approximation for the energy levels λ of $\mathcal{PT}$-symmetric Sturm-Liouville eigenvalue problems. This derivation requires the use of one-turning-point analysis. If a no-turning-point analysis is used one still obtains a good approximation to the high-lying energy levels for fixed coupling constant g. However, the no-turning-point analysis is unable to reproduce the critical points that occur when g and λ are both large. What is most remarkable is that the one-turning-point formula gives an accurate description of the spectrum and critical points even when g and λ are not large.

Particular examples that we have studied included the ix and $i\sin x$ potentials. In these cases we were able to understand the close equality of their respective spectra and why the spectra of the pair of potentials $2ix$ and $i\sin(2x)$ were not equal. In the case of the ix^3 potential the WKB approximation correctly reproduces that higher energy levels, which do not exhibit any critical behavior. There is, however, a low-energy critical point, as seen in Fig. 8, which our WKB approximation does not reproduce. It is an open question whether a two-turning-point approximation would be able to do so.

Acknowledgments

We thank U. Günther and Z. H. Musslimani for useful discussions. CMB is supported by the U.K. Leverhulme Foundation and by the U.S. Department of Energy.

[1] C. M. Bender and S. A. Orszag, *Advanced Mathematical Methods for Scientists and Engineers* (McGraw Hill, New York, 1978), Chap. 10.
[2] U. Günther, F. Stefani, and M. Znojil, J. Math. Phys. **46**, 063504 (2005).
[3] J. Rubinstein, P. Sternberg, and Q. Ma, Phys. Rev. Lett. **99**, 167003 (2007).
[4] K. F. Zhao, M. Schaden, and Z. Wu, Phys. Rev. A **81**, 042903 (2010).
[5] An early use of WKB to locate critical points may be found in C. M. Bender and T. T. Wu, Phys. Rev. Lett. **21**, 406 (1968) and Phys. Rev. **184**, 1231 (1969).
[6] W. D. Heiss, Czech. J. Phys. **54**, 1091 (2004).
[7] B. Dietz, H. L. Harney, O. N. Kirillov, M. Miski-Oglu, A. Richter, and F. Schäfer, Phys. Rev. Lett. **106**, 150403 (2011).
[8] A. Andrianov and A. V. Sokolov, SIGMA **7**, 111 (2011), and references therein.
[9] M. Fagotti, C. Bonatti, D. Logoteta, P. Marconcini, and M. Macucci, Phys. Rev. B **83**, 241406 (R) (2011).
[10] S. Bittner, B. Dietz, U. Günther, H. L. Harney, M. Miski-Oglu, A. Richter, and F. Schäfer, Phys. Rev. Lett. (2012), to appear.
[11] C. M. Bender and R. J. Kalveks, Int. J. Theor. Phys. **50**, 955 (2011).
[12] C. M. Bender, M. V. Berry, and A. Mandilara, J. Phys. A: Math. Gen. **35** L467 (2002); C. M. Bender and P. D. Mannheim, Phys. Lett. A **374**, 1616 (2010).
[13] A. A. Shkalikov, J. Math. Sc. **124**, 2004 (2004).